Proceedings of the ASME 2020
Dynamic Systems and Control Conference
DSCC2020
October 5-7, 2020, Virtual, Online

DSCC2020-3295

DYNAMIC MODELING OF A STEERABLE DRIFTER

Eric Gaskell and Xiaobo Tan

Smart Microsystems Lab
Department of Electrical and Computer Engineering
Michigan State University
East Lansing, MI 48824
Email: gaskelle@msu.edu, xbtan@egr.msu.edu

ABSTRACT

Drifters are energy-efficient platforms for monitoring rivers and oceans. Prior work largely focused on free-floating drifters that drift passively with flow and have little or no controllability. In this paper we propose steerable drifters that use multiple rudders for modulating the hydrodynamic forces and thus maneuvering. A dynamic model for drifters with multiple rudders is presented. Simulation is conducted to examine the behavior of the drifter in two different flow conditions, uniform flow and parabolic flow. When there is no difference in relative flow between the rudders, as in uniform flow, the drifter can only be controlled until its velocity approaches that of the water. However, when present, local flow differentials can be exploited to initiate motion lateral to the ambient flow and control the trajectory of the drifter to some degree. The motion of the drifter is further classified as belonging to one of three major modes, rotational, oscillatory, and stable. The behavior of the drifter in a simulated river was mapped for different rudder angles. Identifying the parameters that induce each mode lays the groundwork for developing a feedback control scheme for the drifter.

INTRODUCTION

Engineers have long sought to improve the monitoring of rivers and waterways. Manually testing water quality requires a significant amount of manpower. The first step toward automation came in 1958, when Edward Cleary [1] discussed a hypothesized system for automatically measuring the quality of the Ohio river. Cleary [2] later wrote in 1962 that six prototype analyz-

ers were made and deployed at strategic fixed points in the river, relaying data to a central logging station. In 1978, Rickert and Hines [3] concluded that each river system will require specialized monitoring to establish cause-effect relationships with water quality issues. Developing a specialized system such as Cleary's tailored to each individual river basin is cost prohibitive. A preferred solution would be a drifter that can be moved between rivers and tributaries, and outfitted with different sensors. The U.S. Geological Survey (USGS) developed a prototype drifter for monitoring acoustically tagged fish in rivers, shown in Figure 1, but this drifter could be outfitted with different sensors tailored to the waterway being measured. Drifters have been used extensively in ocean monitoring. Bishop et al. [4] [5] used two drifting floats to measure the response of marine life to increased iron fertilization from natural and artificial causes. Kieber et al. [6] also employed passive, free-floating drifters to measure photochemical processes and light fluxes in seawater.

Drifters have long been used to measure ocean currents, as free-floating drifters go where the current takes them. GPS technology has greatly expanded the accuracy and amount of data that can be gleaned from drifters. Austin and Atkinson [7] developed low-cost, GPS-tracked drifters in 2004 to make Lagrangian measurements of hydrodynamic forces. Since then, drifters have been a part of several large-scale oceanography experiments [8–12]. Poulain et al. [13] have since attempted to quantify the accuracy of more common drifter types in terms of their slip relative to local currents.

Despite the aforementioned progress in drifter development and applications, prior work has largely focused on passive, free-

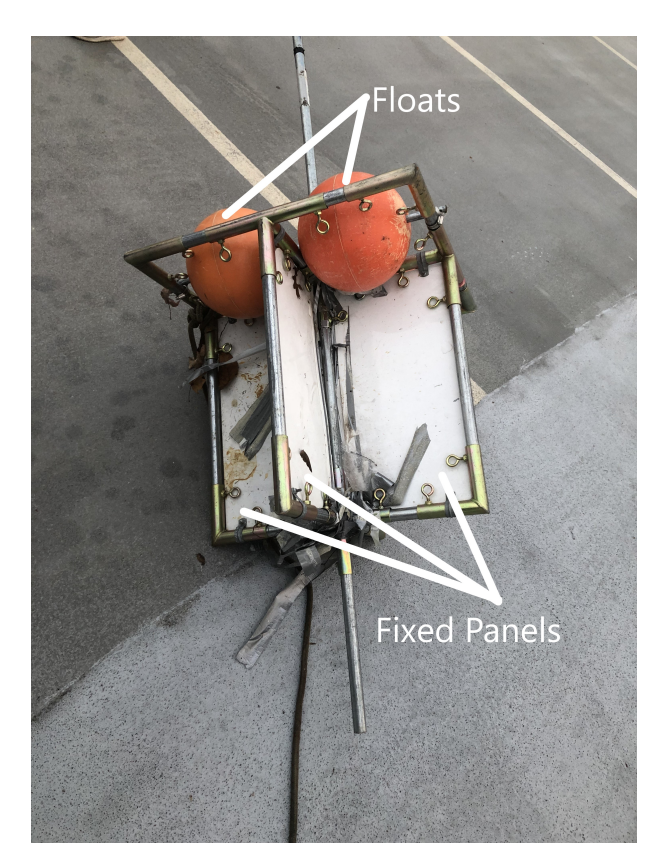


FIGURE 1. A drifter prototype developed by the U. S. Geological Survey for monitoring tagged fish in rivers.

floating drifters that have little controllability. In this paper we propose an active drifter with multiple rudders to enable some degree of control over its trajectory. In order to minimize the energy consumption of controlling the drifter, no powered propulsion is included. However, by using local differences in relative flow between the rudders, the drifter can initiate lateral motion relative to surface currents. This is desirable, especially in rivers, in order to avoid drifting into the riverbank or to achieve sampling in the lateral direction. Instantaneous flows could be estimated similarly to Salumäe and Kruusmaa [14], by using multiple pressure sensors placed strategically on the rudders. From these pressure measurements, the local flow velocity can be estimated for feedback control of the rudders.

A dynamic model of a steerable drifter with multiple rudders is developed. Simulation is further conducted to examine the drifter behavior under different flow conditions with fixed rudder positions. It is found that in uniform flow, regardless of the rudder orientation, the drifter's velocity eventually approaches that of the ambient flow. With no relative velocity between the drifter and the water, the ability to control the drifter with drag forces acting on rudders is diminished. However, in a parabolic flow profile, the behavior of the drifter can follow any of three modes.

The drifter may rotate, which is undesirable. The drifter may also continue to oscillate, swinging back and forth. Although undesirable to remain in this mode, the oscillations may be useful for controlling drifter orientation. The final and most desirable mode in which the drifter may operate is the stable mode, where the drifter's trajectory in both lateral position and angle settles at an equilibrium. These results shed light into the rich behavior of drifter dynamics, and lay groundwork for the design of rudder control to achieve desired maneuvers.

This paper begins with the development of a model of the drifter's linear and rotational dynamics. The drifter is then simulated under uniform flow and in a parabolic flow profile, and the simulation results are summarized. Concluding remarks, including discussion on future work, are provided.

NOMENCLATURE

N - Number of rudders

 l_i - Length of rudder i

 A_i - Area of rudder i

 $A_{i,wet}$ - Wetted area of rudder i

 ρ - Fluid density

 c_d - Rudder shape drag coefficient

 s^0 - Position of drifter, inertial coordinates

 s^1 - Position of drifter, body-fixed frame coordinates

 $\boldsymbol{\Theta}$ - Angle between the inertial reference frame and body-fixed reference frame.

 R_1^0 - Rotation matrix describing axes of the body-fixed frame with respect to the inertial frame.

 H_1^0 - Displacement matrix describing axes of the body-fixed frame with respect to the inertial frame.

 r_i^1 - Position of axis of rudder i in the body-fixed reference frame

 $r_{i,c}^1$ - Position of center of rudder i in body-fixed reference frame

 Φ_i - Angular position of rudder i

 v_f^0 - Flow velocity in the inertial reference frame

 $v_{f,i}^{1}$ - Flow velocity experienced by rudder i in the body-fixed reference frame

 α_i - Angle of attack of rudder i

COORDINATE FRAMES

Figure 2 shows the schematic of the proposed steerable drifter viewed from above and from the side. The drifter has multiple controllable rudders for steerability, and two rudders are sketched in the figure for illustration. The (thin) body of the drifter sits at the surface, and the rudders extend down into the water. In this analysis, we consider the thickness of the drifter body to be negligible, so only the drag forces on the rudders will be considered. The origin of the body-fixed frame (denoted as

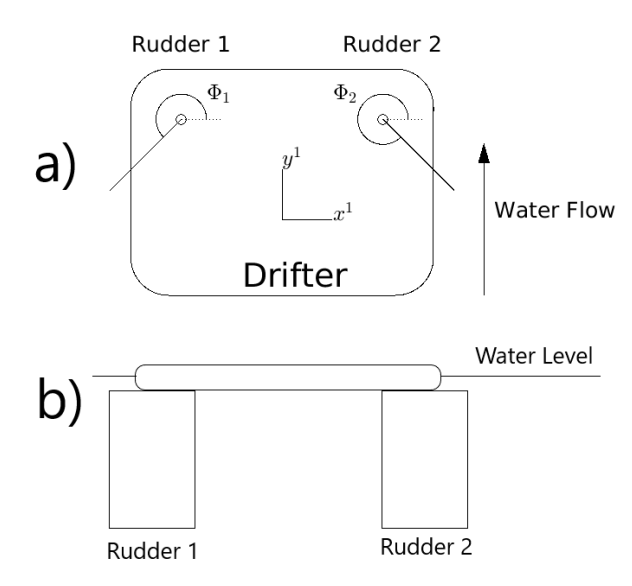


FIGURE 2. Schematic of the proposed steerable drifter: (a) Top view; (b) side view.

 $x^1 - y^1$ frame) is at the center of gravity of the drifter. The rudder angles Φ_1, Φ_2 are measured from the x^1 -axis.

The displacement of the drifter in the inertial frame $(x^0 - y^0)$ frame) is defined by the vector s^0 . The (vertical) z^0 coordinate is defined to be 0 as the motion of the drifter is confined to the horizontal plane. So we simply write s^0 as

$$s^0 = \begin{bmatrix} s^{0,1} \\ s^{0,2} \end{bmatrix},\tag{1}$$

where 1 and 2 in the superscript denotes the x^0 and y^0 components of s^0 , respectively.

Since the drifter is confined to planar motion at the surface, its rotation can be described by a single angle Θ , the angle between the inertial and body frames about the vertical axis. Figure 3 shows the displacement s^0 and angle Θ between the body-fixed frame and the inertial frame. The matrix describing the rotation between the body-fixed frame and the inertial frame is given by

$$R_1^0 = Rot_3(\Theta) = \begin{bmatrix} \cos(\Theta) - \sin(\Theta) \\ \sin(\Theta) & \cos(\Theta) \end{bmatrix}. \tag{2}$$

With the rotation defined by R_1^0 , and the displacement of the drifter in the inertial frame defined by s^0 , the displacement matrix

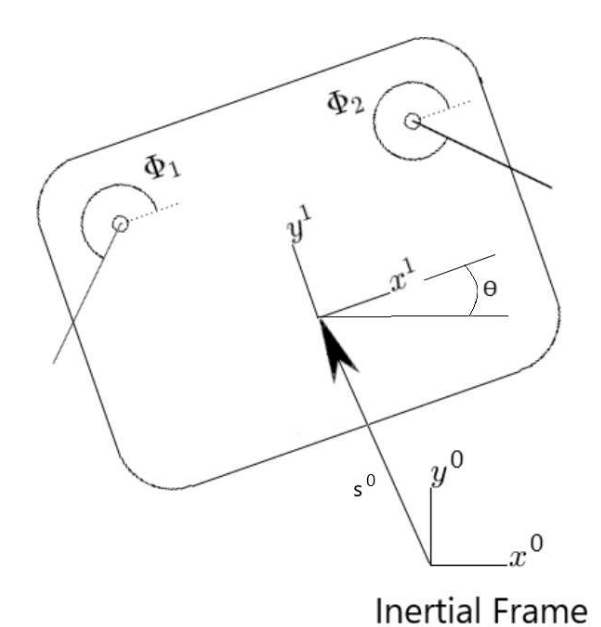


FIGURE 3. Relationship between the inertial reference frame and the body-fixed reference frame.

from the body-fixed frame to the inertial frame H_1^0 can be defined as

$$H_1^0 = \begin{bmatrix} R_1^0 & s^0 \\ 0_{1x2} & 1 \end{bmatrix}. \tag{3}$$

A free vector w^1 in the body-fixed frame can be translated to the inertial frame (w^0) and back through the following operations:

$$w^0 = R_1^0 w^1$$

and

$$w^1 = R_0^1 w^0 = (R_1^0)^T w^0,$$

where T represents the matrix transpose. A fixed vector t^1 in the body-fixed frame can be translated to the inertial frame (t^0) and back through the following operations:

$$\begin{bmatrix} t^0 \\ 1 \end{bmatrix} = H_1^0 \begin{bmatrix} t^1 \\ 1 \end{bmatrix},$$

and

$$\begin{bmatrix} t^1 \\ 1 \end{bmatrix} = H_0^1 \begin{bmatrix} t^0 \\ 1 \end{bmatrix} = (H_1^0)^{-1} \begin{bmatrix} t^0 \\ 1 \end{bmatrix}.$$

DYNAMIC MODELING

First, the positions of the center of each rudder relative to the drifter is determined in the inertial coordinate frame. With rudder i at angle Φ_i , the center of each rudder relative to the drifter in body-fixed frame is located at

$$r_{i,c}^{1} = r_{i}^{1} + \frac{1}{2} \begin{bmatrix} l_{i} \cos(\Phi_{i}) \\ l_{i} \sin(\Phi_{i}) \end{bmatrix}$$
 (4)

The center of each rudder can then be described in the inertial reference frame as follows:

$$\begin{bmatrix} r_{i,c}^0 \\ 1 \end{bmatrix} = H_1^0 * \begin{bmatrix} r_{i,c}^1 \\ 1 \end{bmatrix} = H_1^0 * \begin{bmatrix} r_i^1 + \begin{bmatrix} l_i \cos(\Phi_i) \\ l_i \sin(\Phi_i) \end{bmatrix} \end{bmatrix}$$
(5)

If the flow velocity vector at location s in the inertial frame is given by g(s), the flow velocity $v_{i,f}^0$ at the center location of rudder i, viewed in the inertial reference frame, is expressed by

$$v_{i,f}^{0} = \begin{bmatrix} v_{i,f}^{0,1} \\ v_{i,f}^{0,2} \end{bmatrix} = g\left(r_{i,c}^{0}\right). \tag{6}$$

Next, the velocity of each rudder is determined. As the rudder is only used for steering (instead of propulsion), its rotation can be considered quasi-static with respect to the rotation dynamics of the body. Therefore, one can effectively approximate the angular velocity of rudder *i* by the angular velocity of the drifter. Due to the drifter's confined planar motion, its angular velocity is the same in both the body-fixed and inertial frames:

$$\boldsymbol{\omega}_{i} = \boldsymbol{\omega} = \begin{bmatrix} 0 \\ 0 \\ \dot{\boldsymbol{\Theta}} \end{bmatrix}. \tag{7}$$

The linear velocity of the center of each rudder in the inertial frame is then

$$\begin{bmatrix} v_{i,c}^0 \\ 0 \end{bmatrix} = \begin{bmatrix} \dot{s}^0 \\ 0 \end{bmatrix} + \left(\boldsymbol{\omega} \times \begin{bmatrix} \left(R_1^0 r_{i,c}^1 \right) \\ 0 \end{bmatrix} \right), \tag{8}$$

where \times represents the cross product of vectors. Because ω is restricted to the vertical axis only, this expression can be simplified as

$$v_{i,c}^{0} = \dot{s}^{0} + \begin{bmatrix} 0 & 1 \\ -1 & 0 \end{bmatrix} R_{1}^{0} r_{i,c}^{1} \dot{\Theta}. \tag{9}$$

The velocity of the ambient flow relative to that of the center of rudder i is then

$$v_{i,r}^{0} = v_{i,c}^{0} - v_{i,f}^{0} = \dot{s}^{0} + \begin{bmatrix} 0 & 1 \\ -1 & 0 \end{bmatrix} R_{1}^{0} r_{i,c}^{1} \dot{\Theta} - v_{i,f}^{0}.$$
 (10)

The angle of attack of each rudder, α_i , is the angle between the angular position of the rudder and direction of the relative flow, both expressed in the body-fixed frame:

$$\alpha_i = \angle v_{i,r}^1 - \Phi_i. \tag{11}$$

The wetted surface area is

$$A_{i,wet} = A_i |\sin(\alpha_i)|. \tag{12}$$

The drag force on rudder i, expressed in the body-fixed frame, can be approximated as

$$D_{i}^{1} = \begin{bmatrix} D_{i}^{1,1} \\ D_{i}^{1,2} \end{bmatrix} = -\frac{c_{d}A_{i,wet}\rho}{2} \left\| v_{i,r}^{1} \right\| v_{i,r}^{1}, \tag{13}$$

which yields a force in the direction of the relative flow, proportional to the square of the relative velocity. Note that the relative flow at each point of the rudder varies with the location of the point; for ease of treatment, here we use the relative flow at

the rudder center to approximate the relative flow experienced at each of the rudder.

Because the drag forces are restricted to the horizontal plane, the torque experienced by the drifter is restricted to the vertical only. The torque applied to the drifter due to the drag on rudder i can be expressed as

$$\tau_i = \begin{bmatrix} D_i^1 \\ 0 \end{bmatrix} \times \begin{bmatrix} r_{i,c}^1 \\ 0 \end{bmatrix} = (D_i^1)^T \begin{bmatrix} 0 & 1 \\ -1 & 0 \end{bmatrix} r_{i,c}^1. \tag{14}$$

The translational dynamics of the drifter are then given by

$$\frac{d^2}{dt^2}s^0 = \frac{1}{m}\sum_{i=1}^N R_1^0 D_i^1 = -\frac{c_d \rho}{2m} R_1^0 \sum_{i=1}^N A_{i,wet} \left\| v_{i,r}^1 \right\| v_{i,r}^1, \tag{15}$$

where *m* represents the added mass of the drifter.

The rotational dynamics of the drifter can be expressed as

$$\ddot{\Theta} = \frac{1}{I} \sum_{i=1}^{N} \left(D_i^1 \right)^T \begin{bmatrix} 0 & 1 \\ -1 & 0 \end{bmatrix} r_{i,c}^1$$

$$= -\frac{c_d \rho}{2I} \sum_{i=1}^{N} A_{i,wet} \left\| v_{i,r}^1 \right\| \left(v_{i,r}^1 \right)^T \begin{bmatrix} 0 & 1 \\ -1 & 0 \end{bmatrix} r_{i,c}^1, \tag{16}$$

where *I* denotes the added inertia of the drifter.

For a 2-rudder drifter with rudders of equal area, $A_i = A$, the acceleration of the drifter can be written as

$$\dot{s}^{0} = -\frac{c_{d}\rho A}{2m}R_{1}^{0} \left[\left| \sin \left(\angle v_{1,r}^{1} - \Phi_{1} \right) \right| \left\| v_{1,r}^{1} \right\| v_{1,r}^{1} + \left| \sin \left(\angle v_{2,r}^{1} - \Phi_{2} \right) \right| \left\| v_{2,r}^{1} \right\| v_{2,r}^{1} \right], \quad (17)$$

and the rotational acceleration of such a drifter can be expressed as

$$\ddot{\Theta} = -\frac{c_{d}\rho A}{2I} \left[\left| \sin\left(\angle v_{1,r}^{1} - \Phi_{1}\right) \right| \left\| v_{1,r}^{1} \right\| \left(v_{1,r}^{1}\right)^{T} \begin{bmatrix} 0 & 1 \\ -1 & 0 \end{bmatrix} r_{1,c}^{1} \right.$$

$$+ \left| \sin\left(\angle v_{2,r}^{1} - \Phi_{2}\right) \right| \left\| v_{2,r}^{1} \right\| \left(v_{2,r}^{1}\right)^{T} \begin{bmatrix} 0 & 1 \\ -1 & 0 \end{bmatrix} r_{2,c}^{1} \right].$$

$$(18)$$

SIMULATION RESULTS

The drifter is simulated for two different flow conditions, a uniform and parabolic flow. First, the behavior of a two-rudder drifter shown in Figure 2 is modeled under uniform flow conditions. The drifter starts at $s^0 = \begin{bmatrix} -1 & 0 \end{bmatrix}^T$, and the rudders remained at a fixed angle relative to the drifter. For $\Phi_1 \in [\pi, \frac{3\pi}{2}]$ and $\Phi_2 \in [\frac{-\pi}{2}, 0]$, all combinations of rudder angles simulated eventually reach a stable equilibrium. As the drifter's velocity approaches that of the ambient flow, the drag forces acting on the center of each rudder approach 0. Thus, the controllability of the drifter in uniform ambient flow is limited once it reaches the steady state.

If present, aerodynamic drag will prevent the drifter's velocity from approaching the velocity of the ambient flow. For this analysis, the effect of aerodynamic drag is considered insignificant compared to the hydrodynamic forces present. Ongoing research is being conducted examining the effect of aerodynamic drag on steerable drifters.

Next, the drifter is modeled in the flow profile shown in Figure 4. The longitudinal (y^0 axis) velocity in the inertial frame varies with lateral (x^0 axis) position. This velocity profile is chosen to simulate a simplified river. The local difference in flow velocity between the rudders causes the drifter to behave in one of three main modes, depending on the rudder angles of the drifter.

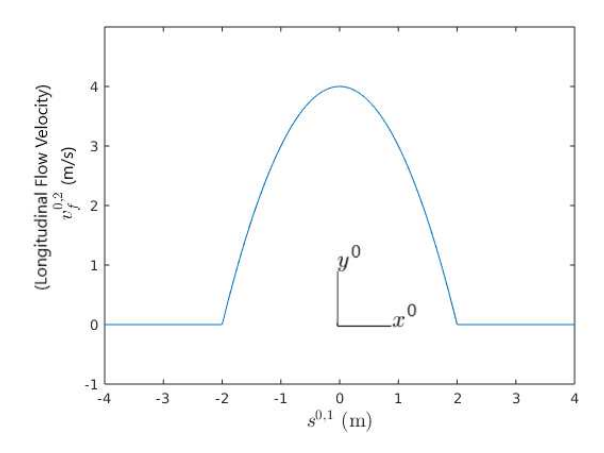


FIGURE 4. Parabolic flow profile in the lateral direction of the simulated river. The flow is assumed to be constant along the longitudinal direction and zero in the lateral direction.

The first mode, shown in Figure 5, is rotary behavior. In this mode, Θ varies monotonically, representing continuous rotation of the drifter. The lateral position of the drifter varies periodically as the drifter rotates, and remains bounded. This behavior is undesirable for controlling the drifter.

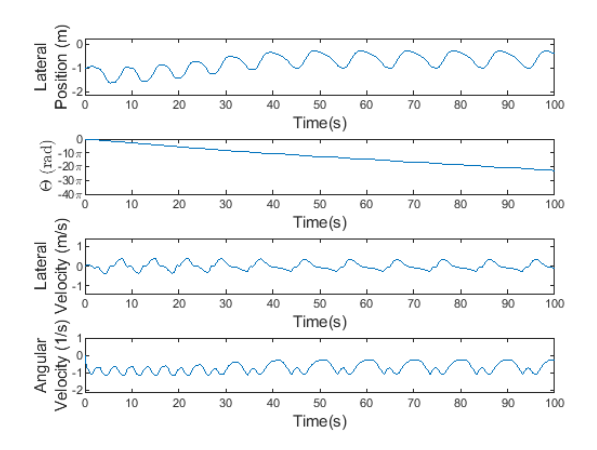


FIGURE 5. Rotary behavior of the drifter under parabolic flow.

The second mode, shown in Figure 6, is oscillatory behavior. In this mode, Θ and the lateral position vary periodically, corresponding to the drifter swinging back and forth. Although generally undesirable, this behavior could be exploited to re-orient the drifter.

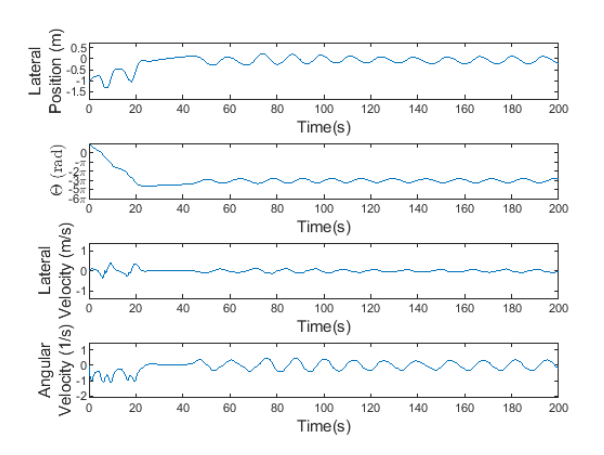


FIGURE 6. Oscillatory behavior of the drifter under parabolic flow. Note that the drifter initially exhibits rotation before oscillating.

The final mode of the drifter observed is stable behavior, shown in Figure 7. In this mode, the drifter tends toward a stable trajectory in both lateral position and angle. This mode is the most desirable for controlling the drifter's behavior.

The rudder angles Φ_1 and Φ_2 that result in each mode are further mapped in Figure 8. Some combinations of rudder angles resulted in mixed behavior, transitioning from one mode to another. In this case, the behavior of the drifter is qualified as

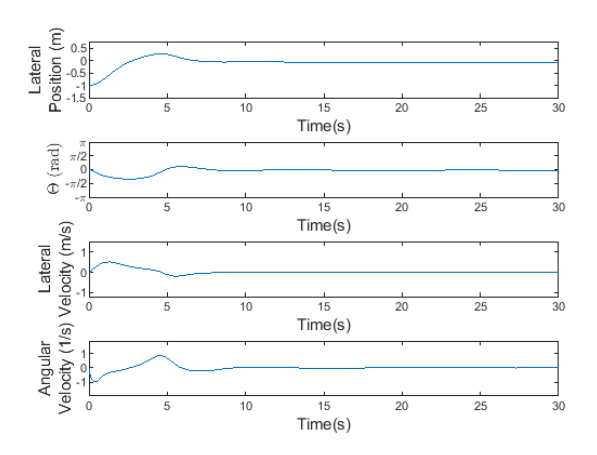


FIGURE 7. Stable behavior of the drifter under parabolic flow.

the final behavior mode. The asymmetry of the map is due to the drifter not starting in the center of the river, and instead starting at $s^0 = \begin{bmatrix} -1 & 0 \end{bmatrix}^T$.

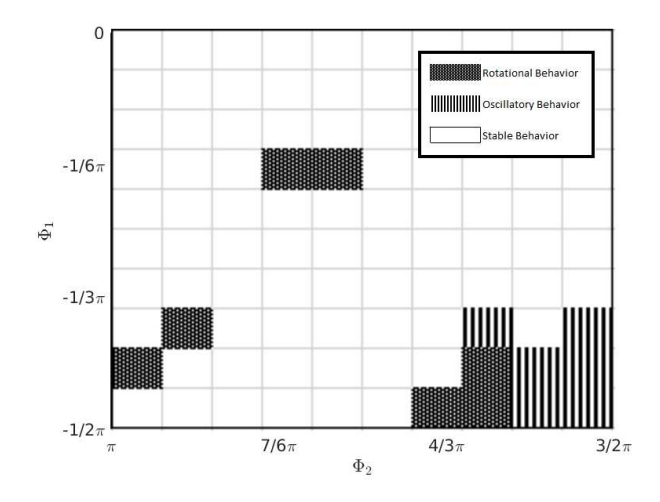


FIGURE 8. Configuration-space map of drifter behavior

CONCLUSION

This paper proposed a steerable drifter for monitoring waterways and their ecosystems. A dynamic model of a steerable drifter with multiple rudders was developed and its behavior was then simulated under uniform and parabolic ambient flow. Under parabolic flow, three major behavior modes were identified (rotational, oscillatory, and stable). These behavior modes were then qualitatively mapped against rudder angles. Ongoing research

into steerable drifters is being conducted, including further analysis into the behavior modes and their stability, development of feedback control schemes, and fabrication and testing of a prototype drifter.

ACKNOWLEDGMENT

This work was supported by the National Science Foundation (IIS 1715714, IIS 1848945).

REFERENCES

- [1] Cleary, E. J., 1958. "Development of a robot system". *Journal (American Water Works Association)*, *50*(9), pp. 1219–1222
- [2] Cleary, E. J., 1962. "Robot monitor system for the ohio valley". *Journal (American Water Works Association)*, **54**(11), pp. 1347–1352.
- [3] Rickert, D. A., and Hines, W. G., 1978. "River quality assessment: Implications of a prototype project". *Science*, **200**(4346), pp. 1113–1118.
- [4] Bishop, J. K. B., Davis, R. E., and Sherman, J. T., 2002. "Robotic observations of dust storm enhancement of carbon biomass in the north pacific". *Science*, 298(5594), pp. 817– 821.
- [5] Bishop, J. K. B., Wood, T. J., Davis, R. E., and Sherman, J. T., 2004. "Robotic observations of enhanced carbon biomass and export at 55s during sofex". *Science*, 304(5669), pp. 417–420.
- [6] Kieber, D. J., Yocis, B. H., and Mopper, K., 1997. "Free-floating drifter for photochemical studies in the water column". *Limnology and Oceanography*, 42(8), pp. 1829–1833.
- [7] Austin, J., and Atkinson, S., 2004. "The design and testing of small, low-cost gps-tracked surface drifters". *Estuaries*, **27**(6), pp. 1026–1029.
- [8] Ohlmann, J. C., 2011. "Drifter observations of small-scale flows in the philippine archipelago". *Oceanography*, **24**(1), pp. 122–129.
- [9] Brushett, B., King, B., and Lemckert, C., 2011. "Evaluation of met-ocean forecast data effectiveness for tracking drifters deployed during operational oil spill response in australian waters". *Journal of Coastal Research*, pp. 991–994.
- [10] Spencer, D., Lemckert, C., Yu, Y., Gustafson, J., Lee, S., and Zhang, H., 2014. "Quantifying dispersion in an estuary: A lagrangian drifter approach". *Journal of Coastal Research*, pp. 29–34.
- [11] Hormann, V., Centurioni, L. R., Mahadevan, A., Essink, S., D'Asaro, E. A., and Kumar, B. P., 2016. "Variability of near-surface circulation and sea surface salinity observed from lagrangian drifters in the northern bay of bengal dur-

- ing the waning 2015 southwest monsoon". *Oceanography*, **29**(2), pp. 124–133.
- [12] Lee, J., Kim, D. H., Lee, S., and Lee, J. L., 2016. "Lagrangian observation of rip currents at haeundae beach using an optimal buoy type gps drifter". *Journal of Coastal Research*, pp. 1177–1181.
- [13] Poulain, P.-M., Bussani, A., Gerin, R., Jungwirth, R., Mauri, E., Menna, M., and Notarstefano, G., 2013. "Mediterranean surface currents measured with drifters: From basin to subinertial scales". *Oceanography*, 26(1), pp. 38–47.
- [14] Salumäe, T., and Kruusmaa, M., 2013. "Flow-relative control of an underwater robot". *Proceedings: Mathematical, Physical and Engineering Sciences*, **469**(2153), pp. 1–19.